RESEARCH PAPER

Luteolin and Tangeretin Synergistically Trigger Mitochondrial Apoptosis Via Dual Egfr/Her2 Suppression In Her2-Overexpressing Breast Cancer

Jaggareddygari Shruthi Reddy[1] and Kumaraswamy Gandla[2*]

[1]*Department of Pharmacology, Chaitanya Deemed to be University, Hyderabad, Telangana-500075, India*
[2*]*Department of Pharmacy, Chaitanya Deemed to be University, Hyderabad, Telangana-500075, India*
[*]***Corresponding author:*** *Prof. Kumaraswamy Gandla, Dean & BoS Chairperson, nDepartment of Pharmacy, Chaitanya Deemed to be University, Hyderabad, Telangana,500075, India*
drkumaraswamygandla@gmail.com

Received: 16th Dec, 2025; Revised: 8th Feb 2026; Accepted: 12th Feb, 2026; Available Online: 28th Feb, 2026

ABSTRACT
HER2-overexpressing breast cancers exhibit aggressive progression driven by aberrant epidermal growth factor receptor (EGFR) and epidermal growth factor receptor 2 (HER2) signaling.Natural flavonoids, such as luteolin and tangeretin, possess anticancer potential; however, their combined mechanistic effects on HER2-driven tumors remain unexplored.This study aimed to evaluate the synergistic antiproliferative activity of luteolin and tangeretin and elucidate their mechanistic involvement in EGFR/HER2 suppression and mitochondrial apoptosis in HER2-positive breast cancer cells. Cytotoxicity was assessed using the MTT [3-(4,5-dimethylthiazol-2-yl)-2,5-diphenyltetrazolium bromide] assay in SKBR3, BT-474, HER2-negative MDA-MB-231, and non-tumorigenic MCF-10A cells. Synergy was quantified using the Chou–Talalay method. Apoptosis was evaluated using Acridine Orange/Ethidium Bromide fluorescence, DNA fragmentation, caspase-3/7 and caspase-9 activities, and JC-1 mitochondrial membrane potential were analyzed.EGFR/HER2 kinase inhibition was measured using phosphorylation-specific In vitro assays, and mechanistic signaling alterations were confirmed via western blotting. The combination of luteolin and tangeretin showed potent synergistic cytotoxicity in SKBR3 (IC_{50} = 3.21 ± 0.28 μM; CI_{50} = 0.351) and BT-474 cells (IC_{50} = 5.69 ± 0.47 μM; CI_{50} = 0.782), surpassing the effects of single agents and approaching that of lapatinib.Combination-treated cells displayed markedly higher late apoptosis (SKBR3:48.8 ± 3.6%; BT-474:49.7 ± 3.5%), extensive DNA laddering, >3-fold increase in caspase-9 and caspase-3/7 activities, and significant mitochondrial depolarization.In vitro kinase assays confirmed robust inhibition of EGFR and HER2 phosphorylation, consistent with the downstream suppression of PI3K/Akt signaling.No significant cytotoxicity or mitochondrial disruption was observed in either MCF-10A or MDA-MB-231 cells. In conclusion, luteolin and tangeretin synergistically inhibit EGFR/HER2 signaling and selectively activate intrinsic mitochondrial apoptosis in HER2-overexpressing breast cancer cells, supporting their potential as safe, low-toxicity dual-targeted therapeutic candidates.

Keywords: Luteolin, Tangeretin, HER2-overexpressing breast cancer, EGFR/HER2 inhibition, Mitochondrial apoptosis, PI3K/Akt signaling
How to cite this article: Reddy JS, Gandla K. Luteolin and Tangeretin Synergistically Trigger Mitochondrial Apoptosis Via Dual EGFR/HER2 Suppression in HER2-Overexpressing Breast Cancer. Int J Drug Deliv Technol. 2026;16(18s): 999-1012. DOI: 10.25258/ijddt.16.18s.113
Source of support: Nil.
Conflict of interest: None

1. INTRODUCTION

Breast cancer is the most frequently diagnosed malignancy and the leading cause of cancer-related mortality among women worldwide [1]. Among its molecular subtypes, HER2-positive breast cancer is characterized by gene amplification and overexpression of the human HER2, leading to aggressive tumor biology, rapid disease progression, and poor clinical outcomes [2]. HER2 overexpression hyperactivates multiple downstream signaling cascades, particularly the PI3K/AKT and MAPK pathways, which drive uncontrolled proliferation, survival, and therapy resistance [3]. Despite the clinical success of HER2-targeted therapies such as trastuzumab, pertuzumab, and lapatinib, intrinsic and acquired resistance remains a major obstacle, often mediated by compensatory activation of EGFR, PI3K mutations, HER2 truncations, and epigenetic reprogramming [4,5]. Thus, innovative therapeutic strategies that can simultaneously modulate HER2 and EGFR signaling and restore apoptotic sensitivity are urgently required.

Natural flavonoids have garnered substantial interest as multi-target anticancer agents owing to their pleiotropic activities, safety profiles, and ability to modulate oncogenic signaling networks [6]. Luteolin, a dietary flavone, exhibits antiproliferative, anti-inflammatory, and pro-apoptotic properties across diverse cancer models, partly through suppression of PI3K/AKT, NF-κB, and

**Author for Correspondence: drkumaraswamygandla@gmail.com*

tyrosine kinase signaling [7].Tangeretin, a polymethoxylated citrus flavone, has demonstrated chemopreventive and anticancer activities, including induction of apoptosis, cell cycle arrest, and inhibition of metastatic signaling[8]. However, their collective impact on HER2-addicted breast cancers and their potential as synergistic modulators of receptor tyrosine kinase signaling remain unexplored.Given the complex interplay between EGFR and HER2 heterodimerization in maintaining oncogenic signaling, dual inhibition of these receptors represents a promising therapeutic strategy for counteracting resistance mechanisms [9]. Additionally, mitochondrial dysfunction, particularly loss of mitochondrial membrane potential (ΔΨm), cytochrome c release, and caspase activation, constitutes a critical pathway for restoring apoptosis in HER2-driven malignancies [10]. However, the ability of flavonoid combinations to simultaneously induce mitochondrial apoptosis while suppressing EGFR and HER2 activity has not been systematically investigated.

In this study, we evaluated the synergistic anticancer potential of luteolin and tangeretin in HER2-overexpressing breast cancer cell lines (SKBR3 and BT-474). We employed a comprehensive experimental workflow, including cytotoxicity profiling, combination index analysis, AO/EB fluorescent apoptosis imaging, DNA fragmentation, caspase-3/7 and caspase-9 activation, mitochondrial membrane potential assessment, and western blot analysis of EGFR/HER2 and downstream signaling. This study aimed to determine whether luteolin and tangeretin, when combined, exert superior anticancer effects through the coordinated suppression of EGFR/HER2 signaling and activation of the mitochondrial apoptotic pathway. Our findings provide strong mechanistic evidence supporting the use of this flavonoid combination as a promising dual-targeted therapeutic strategy for HER2-positive breast cancer.

2. MATERIALS AND METHODS

2.1. Cell Culture

HER2-overexpressing breast cancer cell lines (SKBR3 and BT-474), HER2-negative breast cancer cells (MDA-MB-231), and non-tumorigenic mammary epithelial cells (MCF-10A) were obtained from the Centre for Cellular and Molecular Biology (CCMB), India). Cells were maintained at 37°C in a humidified incubator with 5% CO_2. SKBR3 and BT-474 cells were cultured in RPMI-1640 medium supplemented with 10% fetal bovine serum (FBS), 1% penicillin–streptomycin, and 1% L-glutamine. MCF-10A cells were grown in DMEM/F12 (1:1) medium containing 5% horse serum, 20 ng/mL EGF, 10 µg/mL insulin, 500 ng/mL hydrocortisone, 100 ng/mL cholera toxin, and 1% penicillin–streptomycin. MDA-MB-231 cells were maintained in DMEM supplemented with 10% FBS and 1% penicillin–streptomycin. All cell lines were subcultured to 70–80% confluence using 0.25% trypsin–EDTA and used within 10 passages to ensure phenotypic stability. Cell morphology and confluency were routinely monitored under a phase-contrast microscope to verify healthy growth prior to the experiments.

2.2. Cytotoxicity Evaluation Using the MTT Assay

The cytotoxic effects of luteolin, tangeretin, and their 1:1 molar combination (L+T) were assessed using the MTT [3-(4,5-dimethylthiazol-2-yl)-2,5-diphenyltetrazolium bromide] assay in SKBR3 and BT-474 cells, MDA-MB-231 cells, and non-tumorigenic MCF-10A cells[11]. Cells were seeded into 96-well plates at a density of 5 x 10^3 cells/well in 100 µL of complete medium and allowed to adhere for 24 h at 37°C in a humidified 5% CO_2 environment. After attachment, the cells were exposed to increasing concentrations (0–25 µM) of luteolin, tangeretin, their 1:1 combination, or lapatinib (positive control) for 48 h. All test compounds were dissolved in DMSO, and the final solvent concentration was maintained below 0.1% in all the wells. Untreated and vehicle controls (0.1% DMSO) were included for normalization.Following drug exposure, 20 µL of MTT solution (5 mg/mL in PBS) was added to each well and incubated for 4 h to allow for the formation of formazan. The supernatant was carefully removed, and the resulting crystals were dissolved in 150 µL DMSO. Absorbance was measured at 570 nm using a microplate reader. Cell viability was expressed as a percentage of untreated controls, and IC_{50} values were calculated by nonlinear regression using GraphPad Prism (version 7.0).

2.3. Determination of Combination Index

The synergistic interaction between luteolin and tangeretin was evaluated using the Chou–Talalay method based on median-effect analysis [12]. SKBR3 and BT-474 cells were treated with varying concentrations of luteolin and tangeretin, individually and in fixed-ratio combinations (1:1 molar ratio), across a range of concentrations encompassing their respective IC_{50} values. Cell viability was determined using the MTT assay 48 h after treatment, as described previously.The data were analyzed using CompuSyn software (ComboSyn Inc., Paramus, NJ, USA) to calculate the Combination Index (CI) at the 50% inhibition level (CI_{50}). CI values were interpreted as follows: CI < 1, synergism; CI = 1, additive effect; and CI > 1, antagonism.

2.4. Morphological Analysis of Treated Cells

Cellular morphology was assessed to observe cytotoxic and apoptotic features following the treatment. SKBR3, BT-474, and MCF-10A cells were seeded in 6-well plates at appropriate densities and allowed to adhere for overnight. The cells were then treated for 48 h with luteolin, tangeretin, their combination (1:1 molar ratio), and lapatinib at their respective IC_{50} concentrations. Post-treatment, morphological changes were examined under an inverted phase-contrast microscope at 200x magnification. Images were captured to document the structural alterations. Features such as cell rounding, shrinkage, membrane blebbing, and detachment were evaluated as indicators of apoptosis and cytotoxic responses. Untreated control cells served as a reference for normal morphology, and observations in MCF-10A cells were included to

assess selectivity. Morphological data were used to qualitatively support the findings of the cytotoxicity assays.

2.5. Fluorescence-Based Apoptotic Cell Analysis

Apoptotic cell death was assessed using dual fluorescent staining with Acridine Orange (AO) and Ethidium Bromide (EB) [13].SKBR3, BT-474, and MCF-10A cells were seeded in 6-well plates and treated for 24 h with luteolin, tangeretin, their combination (1:1 molar ratio), and lapatinib at their respective IC_{50} concentrations.Post-treatment, the cells were washed with PBS and stained with a freshly prepared AO/EB solution (100 µg/mL each, mixed in PBS) for 5 min in the dark. Stained cells were immediately visualized under a fluorescence microscope (Ex/Em: ~488/550 nm) at 200x magnification**.** A minimum of 300 cells per sample were analyzed across multiple fields to distinguish viable (green, intact nuclei), early apoptotic (green, condensed/fragmented nuclei), late apoptotic (orange, condensed/fragmented nuclei), and necrotic (orange, intact nuclei) cells.

2.6. DNA Fragmentation Assay

DNA fragmentation, a hallmark of late-stage apoptosis, was assessed in SKBR3, BT-474, and MCF-10A cells after treatment [14]. Cells were seeded in 6-well plates (2 x 10^5 cells/well) and allowed to adhere for 24 h before exposure to luteolin, tangeretin, their 1:1 combination (L + T), and lapatinib at IC_{50} concentrations for 24 h. After treatment, both floating and adherent cells were collected, washed twice with ice-cold PBS, and lysed using 400 µL of lysis buffer containing 10 mM Tris-HCl (pH 7.4), 10 mM EDTA, and 0.5% Triton X-100. Lysates were incubated on ice for 20 min and centrifuged at 12,000 x g for 15 min at 4°C to separate fragmented DNA (supernatant) from intact chromatin (pellet). The supernatant containing fragmented DNA was treated with RNase A (20 µg/mL) for 30 min at 37°C, followed by digestion with proteinase K (100 µg/mL) for 1 h at 55°C. DNA was precipitated by adding 0.5 volume of 5 M NaCl and 2 volumes of ice-cold absolute ethanol, mixed gently, and incubated at −20°C for 1 h. Samples were centrifuged at 12,000 x g for 10 min, and the resulting DNA pellets were washed with 70% ethanol, air-dried, and resuspended in 20 µL TE buffer. DNA samples were resolved on a 1.8% agarose gel containing ethidium bromide and electrophoresed at 80 V for 1.5 h. DNA fragmentation patterns were visualized under UV illumination, where apoptotic cells exhibited characteristic ladder-like bands, whereas intact, high-molecular-weight DNA was observed in the untreated controls and MCF-10A samples**.**

2.7. Caspase-3/7 and Caspase-9 Activity Assays

Caspase activation was quantified to confirm apoptotic induction in SKBR3, BT-474, and MCF-10A cells following methodology[15]. Cells were seeded in 6-well plates at a density of 2 x 10^5 cells/well and allowed to adhere for 24 h before exposure to luteolin, tangeretin, their 1:1 combination (L+T), or lapatinib at IC_{50} concentrations for 24 h. After treatment, the cells were harvested, washed twice with ice-cold PBS, and lysed using 100 µL of the assay kit lysis buffer (Elabscience®, Caspase-3/7: Cat. No. E-CK-A383; Caspase-9: Cat. No. E-CK-A389). Lysates were incubated on ice for 15 min and centrifuged at 12,000 x g for 10 min at 4°C, and the supernatants were collected. Protein concentration was determined using the BCA assay to ensure equal sample loading. For each reaction, 50 µL of the normalized lysate was mixed with 50 µL of caspase reaction buffer containing the specific chromogenic substrates Ac-DEVD-pNA for caspase-3/7 or Ac-LEHD-pNA for caspase-9 in a 96-well plate. The samples were incubated at 37°C for 2 h in the dark, and the absorbance was measured at 405 nm using a microplate reader. Caspase activity is expressed as the fold change relative to that of the untreated controls. SKBR3 and BT-474 cells showed marked caspase-3/7 and caspase-9 activation following combination treatment, whereas MCF-10A cells exhibited no significant increase.

2.8. Mitochondrial Membrane Potential (MMP) (ΔΨm) Assay

MMP (ΔΨm) disruption was assessed using the JC-1 fluorescence assay to determine mitochondrial involvement in apoptosis [16]. SKBR3, BT-474, and MCF-10A cells were seeded in 6-well plates at 2 x 10^5 cells/well and allowed to adhere for 24 h before treatment with luteolin, tangeretin, their 1:1 combination (L+T), or lapatinib at their respective IC_{50} concentrations for 24 h. After treatment, both floating and adherent cells were collected, washed twice with warm PBS, and incubated with 2 µM JC-1 dye (Sigma-Aldrich) prepared in a serum-free medium for 20 min at 37°C in the dark. The cells were then washed gently with PBS to remove excess dye and resuspended in 500 µL of PBS. JC-1 fluorescence was measured immediately using a fluorescence microscope and quantified using a microplate reader (Ex/Em: 488/530 nm for green monomers and 525/590 nm for red J-aggregates). Loss of ΔΨm was indicated by a shift from red (polarized mitochondria) to green (depolarized mitochondria) fluorescence. The ratio of red to green fluorescence was calculated for each sample and expressed relative to the untreated controls. Combination-treated SKBR3 and BT-474 cells displayed a significant reduction in the red/green fluorescence ratio, confirming mitochondrial depolarization, whereas MCF-10A cells showed no appreciable change in this ratio.

2.9. *In vitro* EGFR and HER2 Kinase Inhibition Assay

The direct inhibitory effects of luteolin, tangeretin, and their 1:1 combination (L+T) on EGFR and HER2 kinase activity were evaluated using recombinant human EGFR and HER2 kinase domains and a phosphorylation-specific ELISA-based kinase assay (Abcam, UK) **[17].** Recombinant EGFR (Tyr1068) and HER2 (Tyr1248) kinase proteins were prepared according to the manufacturer's guidelines and equilibrated to room temperature before use. Test compounds were dissolved in DMSO and diluted in the assay buffer to achieve final working concentrations ranging from 0–25 µM, with the DMSO concentration maintained below 0.1%. For each kinase reaction, 50 µL of recombinant EGFR or HER2 enzyme solution was

added to assay wells pre-coated with the kinase substrate, followed by 50 µL of the test compound or lapatinib (positive control). Reactions were initiated by adding ATP to a final concentration of 100 µM and incubating for 30 min at 37°C. The reaction was terminated by washing the wells with wash buffer, and the phosphorylated substrate was detected using HRP-conjugated phospho-specific antibodies supplied with the kit. After a 1 h incubation at room temperature, the wells were washed and developed using TMB substrate for 10–15 min, and the enzymatic reaction was stopped with 2 N sulfuric acid. Absorbance was measured at 450 nm using a microplate reader. Kinase activity was calculated as a percentage of the untreated control (0.1% DMSO), and IC_{50} values for EGFR and HER2 inhibition were determined using nonlinear regression analysis.

2.10. Western Blot Analysis

Western blotting was performed to evaluate the effects of the treatments on EGFR/HER2 signaling, downstream apoptotic markers, and epigenetic regulators in SKBR3 and BT-474 cells[18,19]. Cells were seeded in 6-well plates at 3 x 10^5 cells/well and allowed to adhere for 24 h, then treated with luteolin, tangeretin, their 1:1 combination (L+T), and lapatinib at their respective IC_{50} concentrations for 24 h; untreated cells received medium containing 0.1% DMSO and served as controls. After treatment, the cells were washed twice with ice-cold PBS and lysed in 150–200 µL of RIPA buffer (containing protease and phosphatase inhibitor cocktail) on ice for 30 min. Lysates were clarified by centrifugation at 14,000 x g for 15 min at 4°C, and the supernatants were collected for protein estimation using the BCA assay. Equal amounts of protein (30–40 µg per lane) were mixed with 4x Laemmli sample buffer, boiled for 5 min, and separated on 8–12% SDS–polyacrylamide gels depending on molecular weight. Proteins were transferred onto PVDF membranes using a wet transfer system at 100 V for 90 min. Membranes were blocked with 5% non-fat dry milk or 5% BSA (for phospho-proteins) in Tris-buffered saline containing 0.1% Tween-20 (TBST) for 1 h at room temperature and then incubated overnight at 4°C with primary antibodies against phospho-HER2 (Tyr1248), HER2, phospho-EGFR (Tyr1068), EGFR, phospho-AKT (Ser473), p-AMPK and β-actin (loading control), each diluted in blocking buffer according to the manufacturer's recommendations. After washing three times with TBST, the membranes were incubated with the appropriate HRP-conjugated secondary antibodies for 1 h at room temperature, washed again, and developed using an enhanced chemiluminescence substrate. The bands were visualized using a chemiluminescence imaging system, and densitometric analysis was performed using ImageJ software. Protein expression levels were normalized to β-actin, and phosphorylated proteins were expressed as p-protein/total protein ratios relative to the control.

2.11. Statistical Analysis

All experiments were performed in triplicate using independently cultured cells, and the data are expressed as the mean ± standard deviation (SD). Statistical analyses were performed using GraphPad Prism (version 7.0). Differences between the treatment groups were evaluated using one-way ANOVA, followed by Tukey's post hoc test to determine pairwise significance. For combination treatments, synergistic interactions were assessed using the Chou–Talalay method, and the CI values were generated using CompuSyn software. IC_{50} values for the cytotoxicity and kinase inhibition assays were calculated using nonlinear regression with a sigmoidal dose–response model. Statistical significance was set at $p < 0.05$ for all analyses.

3. RESULTS

3.1. Cytotoxicity Evaluation by MTT Assay

The cytotoxic effects of luteolin, tangeretin, and their 1:1 combination (L+T) were assessed in HER2-positive SKBR3 and BT-474 cells, HER2-negative MDA-MB-231 cells, and non-tumorigenic MCF-10A cells (Figure. 1; Table 1). In SKBR3 cells, the L+T combination demonstrated significantly enhanced antiproliferative activity with an IC_{50} of 3.21 ± 0.28 µM, surpassing luteolin (15.23 ± 1.29 µM), tangeretin (17.66 ± 1.69 µM), and the reference drug lapatinib (3.89 ± 0.32 µM). At 25 µM, the combination reduced viability to 0.11 ± 0.01%, which was markedly lower than the effect of lapatinib (0.68 ± 0.04%). A similar trend was observed in BT-474 cells, where the combination exhibited an IC_{50} of 5.69 ± 0.47 µM, closely approaching the potency of lapatinib (4.57 ± 0.34 µM) and exceeding the efficacy of luteolin (14.85 ± 1.55 µM) and tangeretin (23.69 ± 2.14 µM) alone.In contrast, MCF-10A cells showed minimal susceptibility to all treatments, with IC_{50} values for luteolin, tangeretin, the combination, and lapatinib exceeding 498–743 µM, indicating negligible cytotoxicity, even at the highest tested concentration. HER2-negative MDA-MB-231 cells also displayed limited sensitivity, maintaining >90% viability for all treatments at 25 µM, while lapatinib produced only a modest reduction (87.32% viability). **Overall, the results demonstrate that the combination of luteolin and tangeretin exhibits potent synergistic cytotoxicity selectively in HER2-positive breast cancer cells while sparing HER2-negative and normal epithelial cells.**

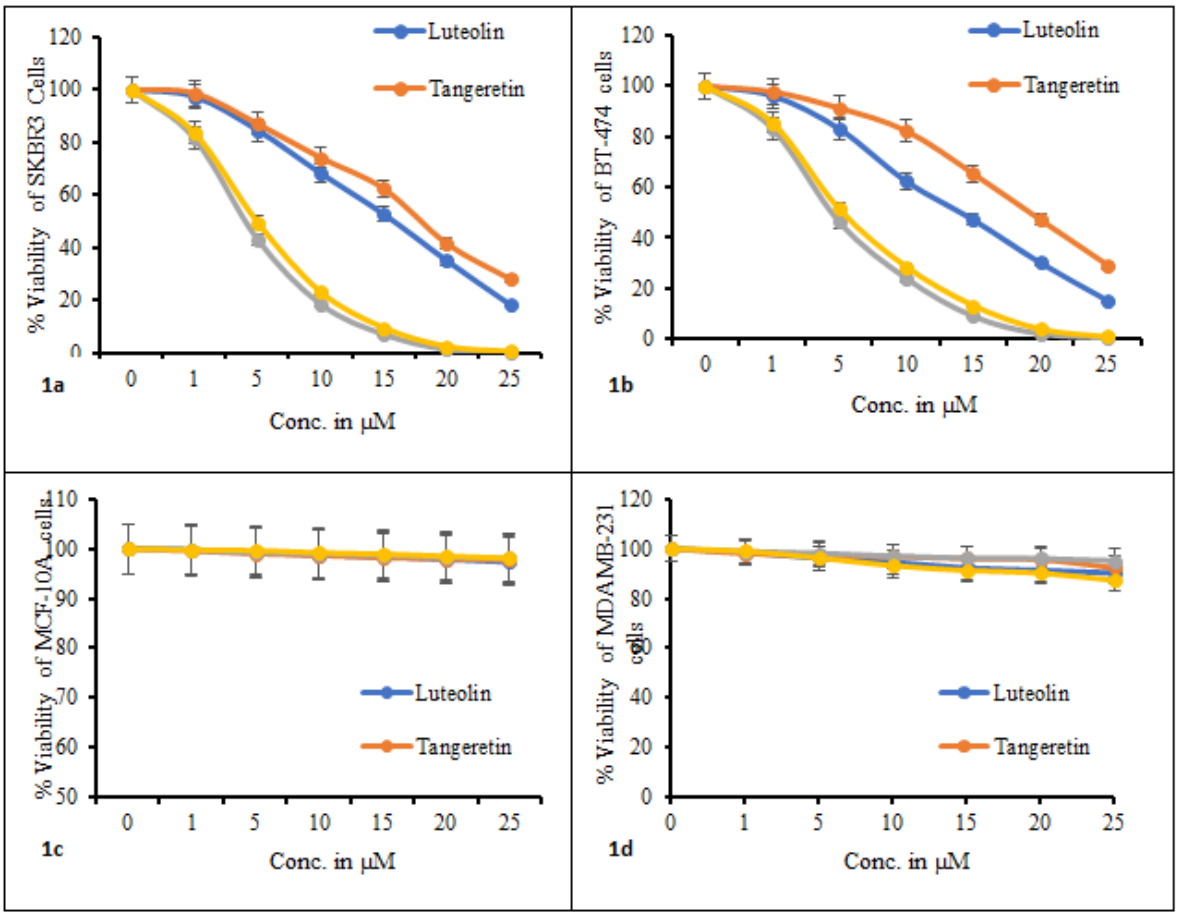

Figure. 1. Cytotoxic effects of luteolin, tangeretin, and their combination (1:1 molar ratio) on (1a) SKBR3, (1b) BT-474, (1c) MCF-10A (1d) MDAMB 231cells after 24 h of treatment, as assessed by MTT assay. Data are presented as mean ± SD of three independent experiments. Statistical significance was determined using one-way ANOVA with Tukey's post hoc test ($p < 0.05$).

Table 1. IC_{50} (µM)of Luteolin and Tangeretin in SKBR3 and BT-474

Cells	Luteolin	Tangeretin	Combination (L+T)	Lapatinib
SKBR3 Cells	15.23 ± 1.29	17.66 ± 1.69	3.21 ± 0.28	3.89 ± 0.32
BT-474 Cells	14.85 ± 1.55	23.69 ± 2.14	5.69 ± 0.47	4.57 ± 0.34
MCF-10A Cells	> 100	> 100	> 100	> 100
MDAMB-231 cells	> 100	> 100	> 100	> 100

3.2. Synergistic Potential of Luteolin and Tangeretin Combination

The synergistic interaction between luteolin and tangeretin in HER2-positive breast cancer cells was quantified using the Chou–Talalay method. The combination produced CI_{50} values of 0.351 in SKBR3 cells and 0.782 in BT-474 cells, demonstrating strong synergy in SKBR3 cells and moderate synergy in BT-474 cells. These synergy values corresponded with the cytotoxicity profiles obtained from the MTT assay, where the combination substantially reduced the IC_{50} to 3.21 ± 0.28 µM in SKBR3 cells and 5.69 ± 0.47 µM in BT-474 cells. In contrast, luteolin and tangeretin alone showed significantly weaker antiproliferative activity, and the efficacy of their combination was comparable to that of lapatinib, a dual EGFR/HER2 inhibitor. These findings confirm that the luteolin–tangeretin combination enhances the cytotoxic potency in HER2-overexpressing breast cancer cells.

3.3. Morphological Assessment

Morphological examination of HER2-positive SKBR3 and BT-474 cells revealed clear treatment-induced alterations following exposure to luteolin, tangeretin, their 1:1 combination (L+T), and lapatinib at IC_{50} concentrations. Untreated controls exhibited normal epithelial morphology, with intact membranes and firm adherence to the culture surface. In contrast, all the treated groups showed characteristic apoptotic features, including cell rounding, shrinkage, membrane blebbing, and partial detachment. Combination treatment produced the most pronounced morphological disruption in both cell lines,

with extensive loss of monolayer integrity and widespread detachment, comparable to or exceeding the effects of lapatinib **(Figure.2).** Luteolin and tangeretin alone caused moderate morphological changes. MCF-10A cells maintained a normal epithelial architecture across all treatments, with no appreciable cytotoxic alterations. These findings visually support the enhanced antiproliferative effect of the combination therapy in HER2-overexpressing breast cancer cells.

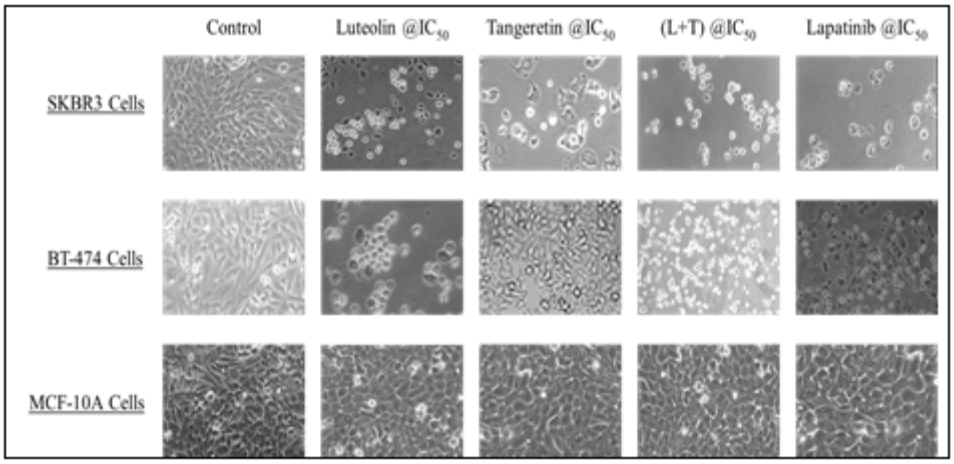

Figure. 2. Morphological assessment of the cytotoxic effects of luteolin, tangeretin, their combination (1:1), and lapatinib in HER2+ breast cancer cell lines SKBR3 and BT-474, and normal breast epithelial cell line MCF-10A. Cells were treated with the respective IC_{50} concentrations for 24 h and visualized using a Zeiss Axiovert phase-contrast microscope (20x magnification).

3.4. Fluorescence-Based Apoptotic Cell Analysis

Dual staining with AO and EB enabled visualization and quantification of apoptotic and necrotic populations in SKBR3, BT-474, and MCF-10A cells following 24 h exposure to luteolin, tangeretin, their 1:1 combination (L+T), or lapatinib at IC_{50} concentrations (Figure.3). SKBR3 cells treated with the combination displayed the strongest apoptotic response, characterized by a markedly reduced viable cell fraction (11.4 ± 0.81%) and a substantial increase in late apoptotic cells (48.8 ± 3.6%). This apoptotic induction exceeded that of lapatinib (41.2 ± 3.2%) and was significantly higher than that observed with luteolin (29.5 ± 2.3%) or tangeretin (19.2 ± 1.4%) alone. A similar pattern was observed in BT-474 cells, where the combination induced 49.7 ± 3.5% late apoptosis, surpassing lapatinib (39.8 ± 2.8%) and single-agent treatments. Necrotic populations were also elevated in combination-treated SKBR3 (17.2 ± 1.3%) and BT-474 (16.4 ± 1.1%) cells. In contrast, MCF-10A cells maintained >98% viability with negligible apoptosis or necrosis across all treatment groups, confirming the minimal cytotoxic impact on normal epithelial cells.

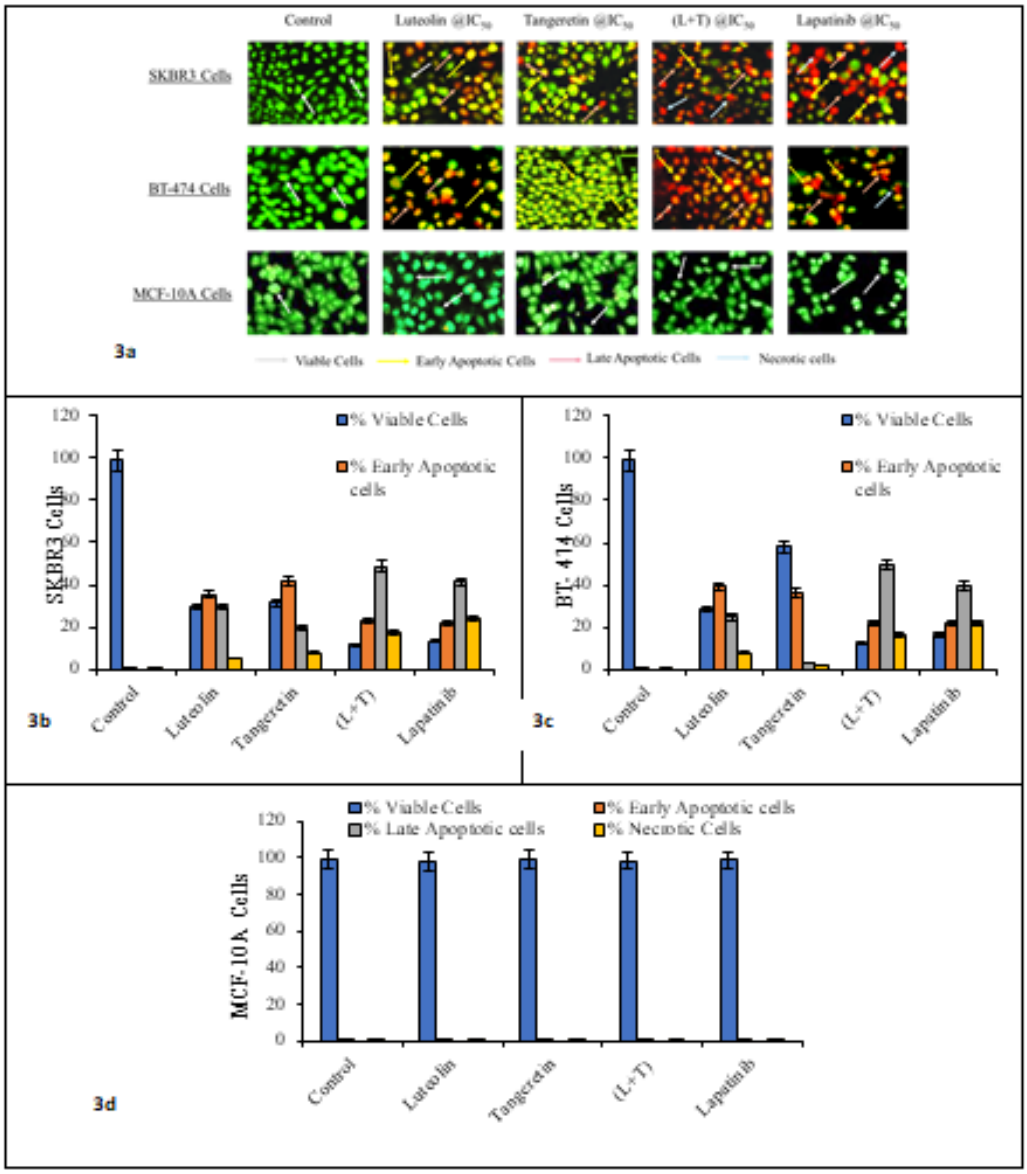

Figure. 3. AO/EB Fluorescence Imaging and Quantitative Apoptosis Assessment; Representative AO/EB-stained images of SKBR3 (3a) and BT-474 (3b) cells following 24 h treatment with luteolin, tangeretin, their 1:1 combination (L+T), and lapatinib at IC_{50} concentrations. Viable cells appeared green, early apoptotic cells yellow-green, late apoptotic cells orange-red, and necrotic cells bright red. The L+T combination produced the strongest apoptotic response, with clear chromatin condensation, membrane blebbing, and increased late apoptotic/necrotic populations compared with individual agents and lapatinib. Scale bar: 50 µm.Quantitative analysis (3c) showed a significant decrease in viable cells and a marked rise in late apoptosis in SKBR3, and BT-474 cells treated with the L+T combination ($p < 0.05$). MCF-10A cells (3d) maintained >98% viability with minimal apoptotic changes across treatments, confirming selective cytotoxicity toward HER2-positive breast cancer cells. Data are expressed as mean ± SD (n = 3).

3.5.DNA Fragmentation Assay

DNA fragmentation patterns were assessed in SKBR3, BT-474, and MCF-10A cells following 24 h of treatment with luteolin, tangeretin, their combination (L+T), and lapatinib at IC_{50} concentrations. In SKBR3 cells (Figure. 4a), the untreated controls showed intact high-molecular-weight DNA with no fragmentation. In contrast, all treated groups exhibited apoptotic laddering, with the combination group exhibiting the most intense and distinct pattern. Consistent with the gel visualization, quantitative analysis revealed markedly elevated DNA fragmentation69.7 ± 3.6% in the L+T combination, higher than luteolin (47.3 ± 2.9%), tangeretin (33.5 ± 1.9%), and lapatinib (63.1 ± 4.5%). A similar trend was observed in BT-474 cells (Figure. 4b), where the combination treatment produced prominent DNA ladders and the highest fragmentation level (66.5 ± 4.1%) compared to luteolin (43.6 ± 2.5%), tangeretin (40.7 ± 3.2%), and lapatinib (61.8 ± 3.8%). In contrast, MCF-10A cells (Figure. 4c) retained intact genomic DNA with negligible laddering for all treatments, corresponding to consistently low fragmentation values (<6%). The overall quantitative

comparison across cell lines is presented in Figure. 4d, which demonstrates significantly higher fragmentation in HER2-positive cells. These results indicate that luteolin and tangeretin, particularly in combination, induce extensive apoptosis-associated DNA degradation selectively in HER2-overexpressing breast cancer cells.

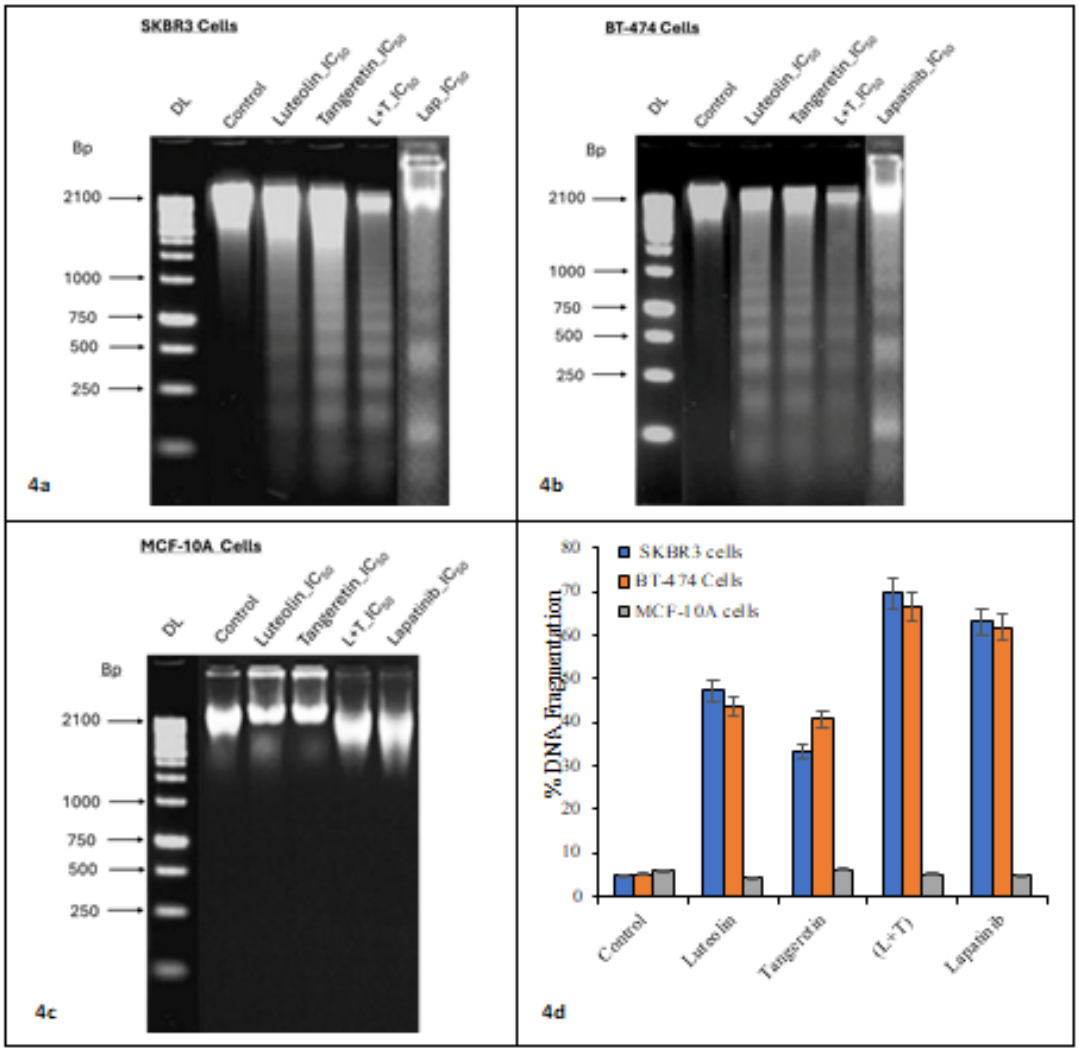

Figure. 4. Representative agarose gel images showing DNA fragmentation in SKBR3 (4a), BT-474 (4b), and MCF-10A (4c) cells after 24 h treatment with luteolin, tangeretin, their combination (L+T), or lapatinib at IC_{50} levels. The controls showed intact genomic DNA, while the treated SKBR3 and BT-474 cells exhibited clear apoptotic laddering, which was most pronounced in the L+T group and comparable to that in the lapatinib group. MCF-10A cells showed no laddering, indicating preserved genomic integrity. (4d) Quantitative DNA fragmentation (%) confirmed maximal fragmentation in the L+T group in both $HER2^+$ lines, significantly higher than that with single agents and absent in normal cells. Data are presented as mean ± SD (n = 3).

3.6. Caspase-3/7 and Caspase-9 Activity

Activation of caspase-3/7 and caspase-9 was quantified in SKBR3, BT-474, and MCF-10A cells following 24 h of treatment with luteolin, tangeretin, their 1:1 combination (L+T), or lapatinib at IC_{50} concentrations. As shown in Figure. 5, SKBR3 cells exhibited a marked increase in caspase activity in all treatment groups, with the combination treatment producing the highest induction (caspase-3/7:6.17-fold, caspase-9:6.27-fold compared to the control). Luteolin and tangeretin alone produced moderate activation (4.08–4.09-fold and 3.42–3.45-fold, respectively), while lapatinib induced strong activity comparable to the combination (5.67–5.64-fold). A similar pattern was observed in BT-474 cells, where the combination treatment elicited 5.46-fold (caspase-3/7) and 5.15-fold (caspase-9) activation, exceeding both single agents and aligning closely with lapatinib treatment.In contrast, MCF-10A cells showed negligible changes in caspase-3/7 and caspase-9 activation across all treatments (1.00–1.25-fold), indicating the absence of apoptosis in non-tumorigenic epithelial cells. These findings confirm that caspase activation is selective for HER2-positive cancer cells and is most pronounced following treatment with the luteolin–tangeretin combination.

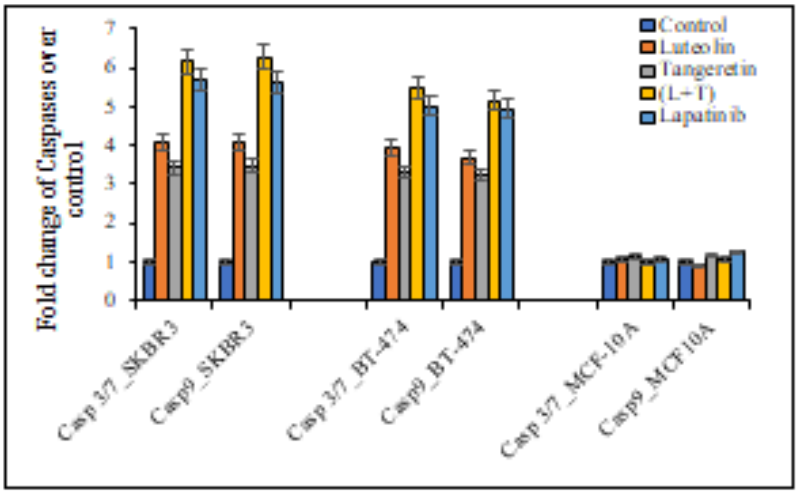

Figure. 5. Caspase-3/7 and Caspase-9 Activation in SKBR3, BT-474, and MCF-10A Cells;Fold-change analysis of caspase-3/7 and caspase-9 activity following 24 h treatment with luteolin, tangeretin, their combination (L+T), or lapatinib at IC_{50} levels. SKBR3 and BT-474 cells exhibited significant activation of both executioner and initiator caspases, with the combination producing the greatest fold increase, consistent with enhanced apoptotic induction. Lapatinib showed comparable activation, whereas the single agents displayed moderate effects. Caspase activity remained unchanged in MCF-10A cells, indicating minimal apoptosis in normal epithelial cells. Data are presented as mean ± SD (n = 3).

3.7. Mitochondrial Membrane Potential (ΔΨm)

Mitochondrial membrane potential was evaluated using the JC-1 assay in SKBR3, BT-474, and MCF-10A cells following 24 h of exposure to luteolin, tangeretin, their 1:1 combination (L+T), or lapatinib at IC_{50} concentrations. As shown in Figure. 6, both SKBR3 and BT-474 cells exhibited a marked reduction in ΔΨm upon treatment, as indicated by the decreased red/green fluorescence ratios. In SKBR3 cells, ΔΨm declined from 17.20 in the control to 9.23 (luteolin), 11.40 (tangeretin), 7.88 (lapatinib), and reached the lowest value with the combination (6.35). A similar trend was observed in BT-474 cells, where ΔΨm decreased from 23.54 (control) to 12.3, 15.9, 10.8, and 9.7 with luteolin, tangeretin, lapatinib, and the combination, respectively. In contrast, ΔΨm remained largely unchanged in MCF-10A cells across all treatments, with values clustering near control levels (18.1–19.2), indicating negligible mitochondrial depolarization in the non-tumorigenic cells.

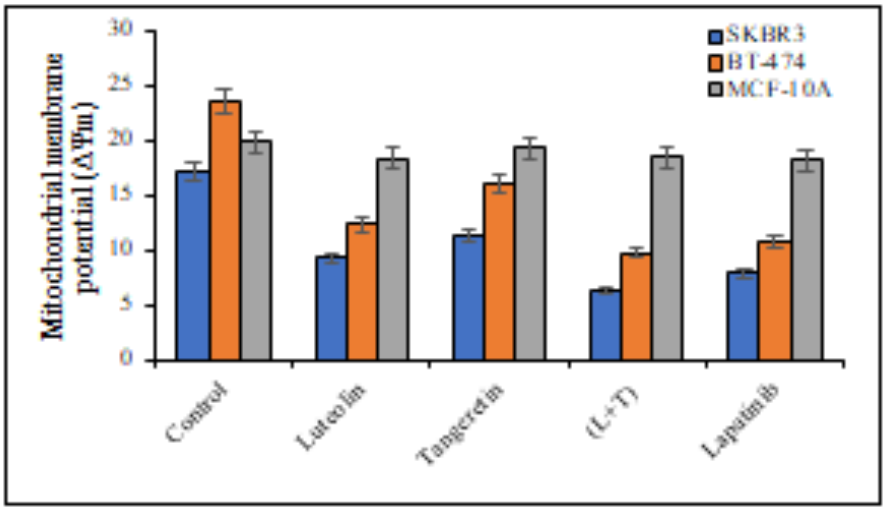

Figure. 6. Mitochondrial Membrane Potential (ΔΨm) Disruption in SKBR3, BT-474, and MCF-10A Cells; JC-1 fluorescence-based assessment of mitochondrial membrane potential following 24 h of treatment with luteolin, tangeretin, their combination (L+T), or lapatinib at IC_{50} concentrations. A significant loss of ΔΨm was observed in SKBR3 and BT-474 cells, with the combination producing the greatest depolarization, comparable to or exceeding that of lapatinib. Single agents induced moderate ΔΨm loss. MCF-10A cells maintained a stable ΔΨmacross all treatments, indicating preserved mitochondrial integrity. Data are expressed as red/green fluorescence ratios (mean ± SD, n = 3).

3.8. In vitroEGFR and HER2 Kinase Inhibition

The inhibitory effects of luteolin, tangeretin, their 1:1 combination (L+T), and lapatinib on recombinant EGFR and HER2 kinase activities were quantified using an ELISA-based kinase inhibition assay. As shown in **Figure.** 7a, EGFR activity decreased in a concentration-dependent manner for all compounds, with the L+T combination exhibiting the greatest inhibition at all tested concentrations. At 100 nM, the combination achieved 97.8 ± 4.8% EGFR inhibition, exceeding the activity of luteolin (81.8 ± 4.7%), tangeretin (77.2 ± 5.6%), and lapatinib (93.3 ± 6.3%) alone. The calculated IC_{50} values further confirmed the superior potency of the combination (18.6 ± 1.1 nM) relative to the single agents (luteolin: 45.2 ± 3.2 nM, tangeretin: 52.7 ± 2.6 nM) and even lapatinib (22.3 ± 1.1nM).A similar inhibitory trend was observed for the HER2 kinase activity (**Figure.** 7b). The L+T combination demonstrated the strongest inhibition, with 98.4% suppression at 100 nM, compared to luteolin (83.2 ± 3.9%), tangeretin (75.1 ± 5.2%), and lapatinib (95.3 ± 4.9%). The IC_{50} for the combination (20.1 ± 1.6 nM) was markedly lower than that of luteolin (49.8 ± 3.9 nM) and tangeretin (55.3 ± 2.7 nM), and comparable to lapatinib (25.7 ± 1.6nM). Comparative IC_{50} values for EGFR and HER2 inhibition across the compounds are summarized in **Figure.**7c, demonstrating the consistently greater potency of the L+T combination.

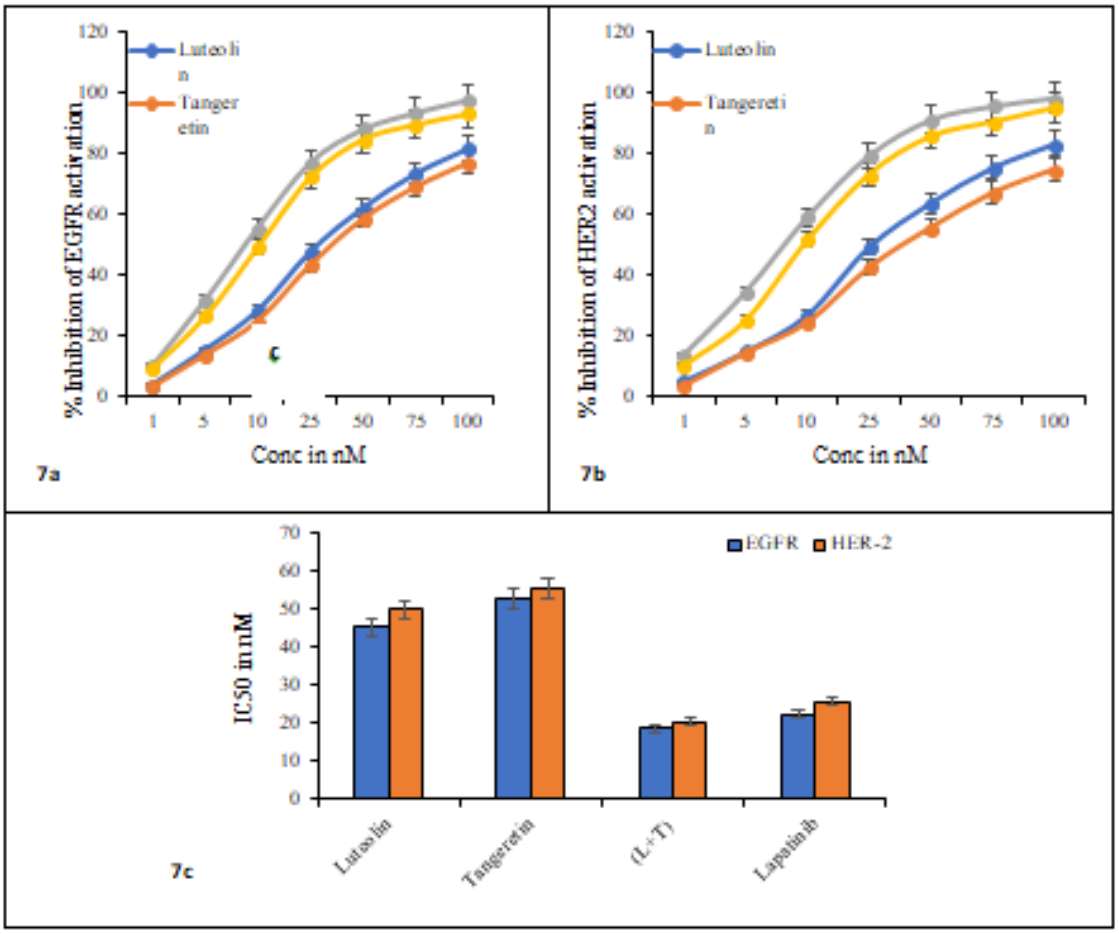

Figure. 7.*In vitro* EGFR and HER2 kinase inhibition by luteolin, tangeretin, their combination (L+T), and lapatinib;(7a) Concentration-dependent inhibition of recombinant EGFR kinase activity. (7b) Concentration-dependent inhibition of recombinant HER2 kinase activity. (7c) Comparative IC_{50} values for EGFR and HER2 inhibition. The L+T combination exhibited the strongest inhibition across all concentrations and significantly lower IC_{50} values than the individual phytochemicals *($p < 0.05$ vs. luteolin and tangeretin)* and comparable or superior inhibition relative to lapatinib. Data are presented as mean ± SD (n = 3).

3.9. Western Blot Analysis of EGFR/HER2 Signaling and Downstream Pathways

Western blot analysis revealed significant modulation of EGFR/HER2 signaling and associated downstream proteins in SKBR3 and BT-474 cells following treatment with luteolin, tangeretin, their combination (L+T), and lapatinib (**Figures** 8a–d).In SKBR3 cells, luteolin and tangeretin moderately reduced phosphorylated EGFR (p-EGFR: 0.43 and 0.59) and phosphorylated HER2 (p-HER2:0.41 and 0.53), while their total EGFR and HER2 levels remained largely unchanged (0.87–0.65). The combination (L+T) induced the strongest suppression of receptor activation, reducing p-EGFR and p-HER2 to 0.35 and 0.29, respectively, comparable to lapatinib (0.39 and

*Author for Correspondence: drkumaraswamygandla@gmail.com

0.33).Similarly, in BT-474 cells, the combination treatment markedly decreased phosphorylation of both receptors (p-EGFR: 0.52; p-HER2: 0.24), exceeding the inhibitory effects of luteolin (0.59; 0.33) and tangeretin (0.72; 0.51), and showing a response similar to lapatinib (0.57; 0.35). The total receptor expression remained near the baseline across all treatments.Downstream signaling markers showed pronounced inhibition in both cell lines. L+T reduced phosphorylated Akt to 0.25 in SKBR3 and 0.31 in BT-474, a stronger inhibition than luteolin, tangeretin, or lapatinib alone. In contrast, AMPK phosphorylation was decreased (0.37 in SKBR3 cells; 0.42 in BT-474 cells), consistent with apoptosis-associated metabolic disruption.Collectively, L+T demonstrated the most effective suppression of p-EGFR, p-HER2, and p-Akt among all treatments, closely approximating or surpassing the effects of lapatinib, while maintaining a minimal effect on total receptor levels.

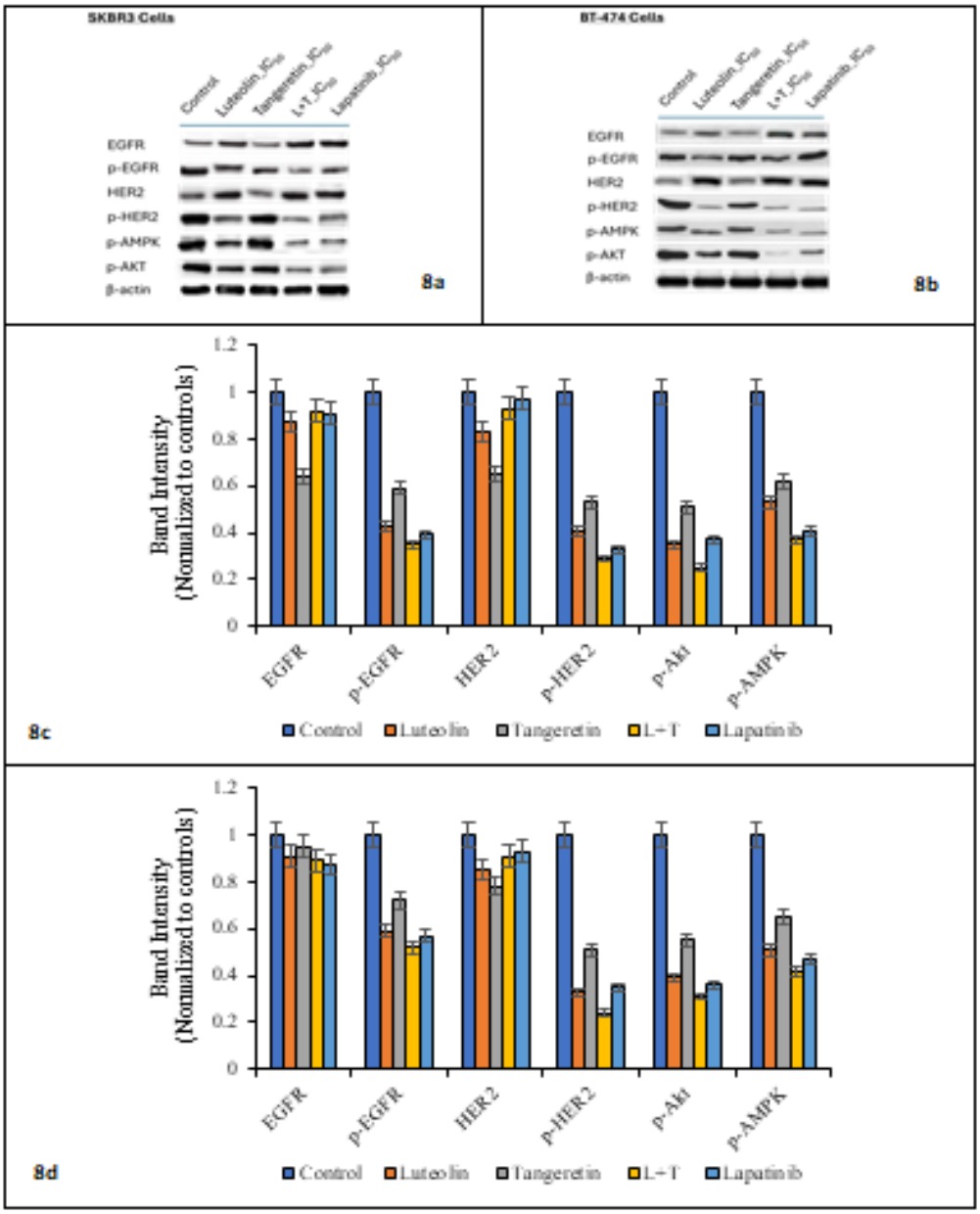

Fig. 8. Western blot analysis of EGFR/HER2 signaling and downstream apoptotic markers in HER2-positive breast cancer cells. Representative blots showing expression of EGFR, p-EGFR, HER2, p-HER2, p-Akt, and p-AMPK in SKBR3 (8a) and BT-474 (8b) cells after 24 h of treatment with luteolin, tangeretin, their combination (L+T), or lapatinib at IC_{50} concentrations. β-actin served as loading control. Quantitative densitometry of SKBR3 (8c) and BT-474 (8d) cells showed that the L+T combination produced the greatest suppression of p-EGFR, p-HER2, and p-Akt levels, comparable to or exceeding lapatinib, while total receptor levels remained largely unchanged. Data are presented as mean ± SD (n = 3), and $p < 0.05$ was considered statistically significant relative to the controls.

4. DISCUSSION

The present study provides comprehensive mechanistic evidence that the combined administration of luteolin and tangeretin exerts a synergistic and selective anticancer effect on HER2-overexpressing breast cancer cells. Across multiple complementary assays, this combination exhibited significantly enhanced cytotoxicity compared to either compound alone, with IC_{50} values approaching or surpassing those of the clinically approved dual EGFR/HER2 inhibitor lapatinib. The strong agreement between MTT-derived IC_{50} reductions and Chou–Talalay synergism indices—particularly the profound synergy in SKBR3 cells (CI_{50} = 0.351)–suggests that the flavonoid combination engages HER2-driven oncogenic dependencies with high mechanistic precision, consistent with prior observations that flavonoids modulate HER2/EGFR signaling and enhance anticancer efficacy in receptor-driven breast cancers[20–22]. Morphological and AO/EB fluorescence-based apoptotic analyses further corroborated this synergistic activity, revealing pronounced apoptotic features, including chromatin condensation, fragmentation, and membrane blebbing, in combination-treated SKBR3 and BT-474 cells. Notably, the magnitude of late apoptosis induced by the combination exceeded that of lapatinib and far surpassed that of single-agent treatments, emphasizing the cooperative engagement of apoptotic signaling pathways. This enhanced apoptotic phenotype was consistent with extensive DNA fragmentation, demonstrating that the combination robustly activates late-stage apoptotic machinery, in line with established apoptotic hallmarks reported in flavonoid-treated carcinoma cells[23]. Crucially, MCF-10A normal epithelial cells exhibited negligible cytotoxicity, minimal apoptosis, and preserved genomic integrity across all assays, confirming the specificity of the combination for HER2-driven oncogenic signaling rather than generalized toxicity, which is a desirable profile also observed in selective flavonoid-based therapeutics [24].

Mechanistic interrogation through caspase activity assays revealed substantial activation of caspase-9 and caspase-3/7, firmly establishing the intrinsic, mitochondria-dependent pathway as the principal mode of cell death in these cells. These biochemical findings were strongly supported by JC-1 assays, which demonstrated profound mitochondrial depolarization exclusively in HER2-positive cells following the combination treatment. The collapse in $\Delta\Psi m$, along with heightened caspase activity and DNA fragmentation, supports a mechanistic model in which the flavonoid combination disrupts mitochondrial homeostasis and lowers the apoptotic threshold in HER2-addicted cancer cells, consistent with canonical mitochondrial apoptotic signaling[25]. and prior reports of flavonoid-mediated mitochondrial destabilization[26]. Upstream analysis through *In vitro* kinase inhibition revealed potent suppression of recombinant EGFR and HER2 activity by the combination, with significantly lower IC_{50} values than those of either compound alone. This dual kinase inhibition is mechanistically meaningful, given the central role of EGFR/HER2 heterodimer signaling in maintaining survival and proliferation in HER2-amplified tumors [27]. Western blot analyses further confirmed the suppression of p-EGFR and p-HER2 in cellular contexts, accompanied by downstream inhibition of p-Akt, a key pro-survival mediator intimately linked to HER2 signaling [28]. This multilayered suppression of receptor-level and PI3K/Akt signaling closely aligns with the observed apoptotic phenotypes, providing a unifying explanation for the synergistic effects of the two flavonoids.

Collectively, these findings establish that luteolin and tangeretin synergize through a dual-mechanism framework: (i) upstream blockade of EGFR/HER2 kinase activation and (ii) downstream activation of intrinsic apoptotic pathways via mitochondrial destabilization, caspase activation, and genomic fragmentation. The selective targeting of HER2-positive cancer cells, coupled with minimal effects on normal epithelial cells and HER2-negative breast cancer cells, underscores the therapeutic potential of this phytochemical combination. These results position the luteolin–tangeretin pair as a compelling candidate for further preclinical development, including in vivo validation and exploration of its potential as a low-toxicity adjunct or alternative to conventional HER2-targeted therapy.

5. CONCLUSION

This study demonstrates that luteolin and tangeretin, when combined in a 1:1 ratio, exert a potent and selective anticancer effect against HER2-overexpressing breast cancer cells through the coordinated inhibition of EGFR/HER2 signaling and activation of intrinsic apoptotic pathways. This combination markedly reduced cell viability, with IC_{50} values substantially lower than those of the individual compounds and comparable to those of the clinically used dual kinase inhibitor lapatinib. Synergy analysis using the Chou–Talalay method confirmed strong synergy, particularly in SKBR3 cells. Complementary morphological, fluorescence-based apoptosis, and DNA fragmentation studies further validated the robust apoptotic response induced by the combination, which significantly exceeded that induced by either luteolin or tangeretin alone. Mechanistically, this combination treatment elicited pronounced mitochondrial depolarization, enhanced caspase-3/7 and caspase-9 activation, and extensive DNA fragmentation, highlighting the activation of the mitochondrial apoptotic cascade. Western blot analysis confirmed the substantial downregulation of phosphorylated EGFR, HER2, and Akt, along with enhanced AMPK activation, demonstrating the simultaneous suppression of oncogenic signaling and metabolic reprogramming. Importantly, this combination exhibited minimal cytotoxicity in MCF-10A normal epithelial cells and HER2-negative MDA-MB-231 cells, highlighting its specificity for HER2-driven tumors. Collectively, these findings establish the luteolin–tangeretin combination as a promising dual EGFR/HER2-

targeted therapeutic strategy capable of selectively inducing mitochondrial apoptosis in HER2-positive breast cancer cells. This synergistic phytochemical pairing warrants further investigation in preclinical *in vivo* models and may serve as a foundation for developing low-toxicity, mechanism-driven anticancer interventions.

ACKNOWLEDGEMENTS
The authors sincerely acknowledge **Chaitanya Deemed to be University,** Hyderabad,for providing the research facilities, technical assistance, and essential infrastructure required to conduct this work.

Financial Support
No external funding was received for the study. All research activities were carried out with the authors' personal financial support.

Conflict of Interest
The authors declare no conflicts of interest associated with this study.

Data Availability Statement
The data supporting the findings of this study are available from the corresponding author upon reasonable request.

Ethics Statement
This study did not involve human participants, animal models, or biological materials that required ethical approval. Hence, no ethical clearance was required.

Informed Consent Statement
This study did not include human participants; therefore, informed consent was not required.

Clinical Trial Registration
This study did not involve any clinical trials and thus did not require clinical trial registration.

Permission to Reproduce Material from Other Sources
Not applicable. No previously published Figure's, tables, or materials were reused in this study.

Author Contributions
J. Shruthi Reddy: Idea discussion, Methodology, Experimental Work, Data Acquisition, Formal Analysis, Investigation, Writing Original Draft Preparation.

Kumaraswamy Gandla: Conceptualization, supervision, validation, critical review, and project administration.

AI-Assisted Language and Editing Statement
AI-assisted language editing tools were used only for grammar and readability improvement.

Abbreviations

EGFR – Epidermal Growth Factor Receptor

HER2 – Human Epidermal Growth Factor Receptor 2

MTT – 3-(4,5-dimethylthiazol-2-yl)-2,5-diphenyltetrazolium bromide

AO – Acridine Orange

EB – Ethidium Bromide

CI – Combination Index

MMP – Mitochondrial Membrane Potential

PI3K – Phosphoinositide 3-kinase

Akt – Protein kinase B

REFERENCES

1. Sung H., Ferlay J., Siegel R.L., et al. Global cancer statistics 2020: GLOBOCAN estimates of incidence and mortality worldwide. *CA Cancer J Clin.* 2021;71(3):209-249.
2. Slamon D.J., Clark G.M., Wong S.G., et al. Human breast cancer: correlation of relapse and survival with amplification of the HER2 oncogene. *Science.* 1987;235(4785):177-182.
3. Pernas S., Tolaney S.M., Winer E.P., Goel S. HER2-positive breast cancer. *Lancet.* 2018;393(10175):174-186.
4. Rexer B.N., Arteaga C.L. Intrinsic and acquired resistance to HER2-targeted therapies. *Nat Rev Clin Oncol.* 2012;9(5):263-274.
5. Cobleigh M.A., Vogel C.L., Tripathy D., et al. Multinational study of trastuzumab therapy for HER2-overexpressing metastatic breast cancer. *J Clin Oncol.* 1999;17(9):2639-2648.
6. Panche A.N., Diwan A.D., Chandra S.R. Flavonoids: an overview. *J Nutr Sci.* 2016;5: e47.
7. Imran M., Rauf A., Abu-Izneid T., et al. Luteolin, a flavonoid, as an anticancer agent: A review. *Biomed Pharmacother.* 2019;112: 108612.
8. Chen J.H., Ho C-T. Antioxidant and antiproliferative activities of citrus flavonoids. *J Agric Food Chem.* 1995;43(9):2709-2713.
9. Moasser M.M. The oncogene HER2: its signaling and transforming functions and its role in human cancer pathogenesis. *Oncogene.* 2007;26(45):6469-6487.
10. Redza-Dutordoir M., Averill-Bates D.A. Activation of apoptosis signaling pathways by reactive oxygen species. *BiochimBiophys Acta.* 2016;1863(12):2977-2992.
11. Hermawan A., et al. Citrus flavonoids for overcoming breast cancer resistance to methotrexate: identification of potential targets of nobiletin and sinensetin. *Cancer Drug Targets.* 2025; (in press).
12. Chou T-C. Drug combination studies and their synergy quantification using the Chou-Talalay method. *Cancer Res.* 2010;70(2):440-446.
13. Ribble D., Goldstein N.B., Norris D.A., Shellman Y.G. A simple technique for quantifying apoptosis in 96-well plates. *BMC Biotechnol.* 2005; 5:12.

14. Lyon C.J., et al. DNA fragmentation assay for apoptosis detection in cultured cells. *Methods Mol Biol.* 2017; 1554:13-22.
15. Slee E.A., Adrain C., Martin S.J. Executioner caspase-3, -6 and -7 perform distinct, overlapping substrate cleavage roles during the demolition phase of apoptosis. *J Biol Chem.* 2001;276(10):7320-7326.
16. Perelman A., Wachtel C., Cohen M., et al. JC-1: alternative excitation wavelengths facilitate mitochondrial membrane potential cytometry. *Cell Death Dis.* 2012;3:e430.
17. Zhang J., Yang P.L., Gray N.S. Targeting cancer with small molecule kinase inhibitors. *Nat Rev Cancer.* 2009;9(1):28-39.
18. Sule R., Abdelrahman H., Sayed S., Mahmoud S. Western blotting (immunoblotting): history, theory, uses and future directions. *BioTechniques.* 2023;74(1):1-14.
19. Mahmood T., Yang P.C. Western blot: technique, theory, and troubleshooting. *N Am J Med Sci.* 2012;4(9):429-434.
20. Lin Y., Shi R., Wang X., Shen H.M. Luteolin, a flavonoid with potential for cancer prevention and therapy. *Curr Cancer Drug Targets.* 2008;8(8):634-646.
21. Lim D.Y., Cho H.J., Kim J., et al. Luteolin decreases IGF-1 and HER2 signaling in breast cancer. *Carcinogenesis.* 2014;35(2):240-248.
22. Kanno S., Shouji A., Asou K., et al. Flavonoids inhibit EGFR/HER2 phosphorylation in cancer cells. *Cancer Lett.* 2004;214(2):167-175.
23. Elmore S. Apoptosis: a review of programmed cell death. *ToxicolPathol.* 2007;35(4):495-516.
24. Harada K., Ferdous T., Ueda S., et al. Selective apoptotic effects of flavonoids in HER2-positive breast cancer. *Mol Carcinog.* 2018;57(1):106-118.
25. Green D.R., Llambi F. Cell death signaling through the mitochondria. *Cold Spring Harb Perspect Biol.* 2015;7(12): a006080.
26. Kong Y., Chen J., Zhou Z., et al. Flavonoids trigger mitochondrial depolarization and intrinsic apoptosis. *J Cell Mol Med.* 2019;23(1):684-697.
27. Moasser M.M. The oncogene HER2: its signaling, therapeutic targeting, and resistance mechanisms. *Oncologist.* 2007;12(1):39-49.
28. Baselga J., Swain S.M. Novel anticancer targets: HER2 and the PI3K/Akt pathway. *Nat Rev Cancer.* 2009;9(7):463-475.